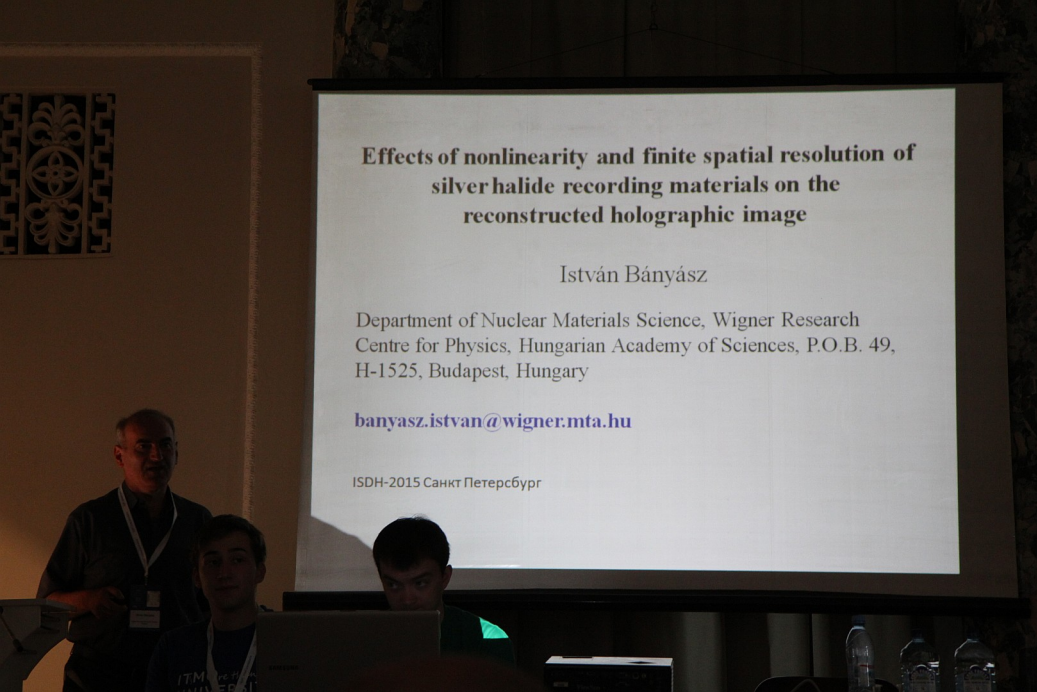
Effects of nonlinearity and finite spatial resolution of silver halide recording materials on the reconstructed holographic image
István Bányász
Department of Nuclear Materials Science, Wigner Research Centre for Physics, Hungarian Academy of Sciences, P.O.B. 49, H-1525, Budapest, Hungary
banyasz.istvan@wigner.mta.hu
ISDH-2015 Санкт Петерсбург

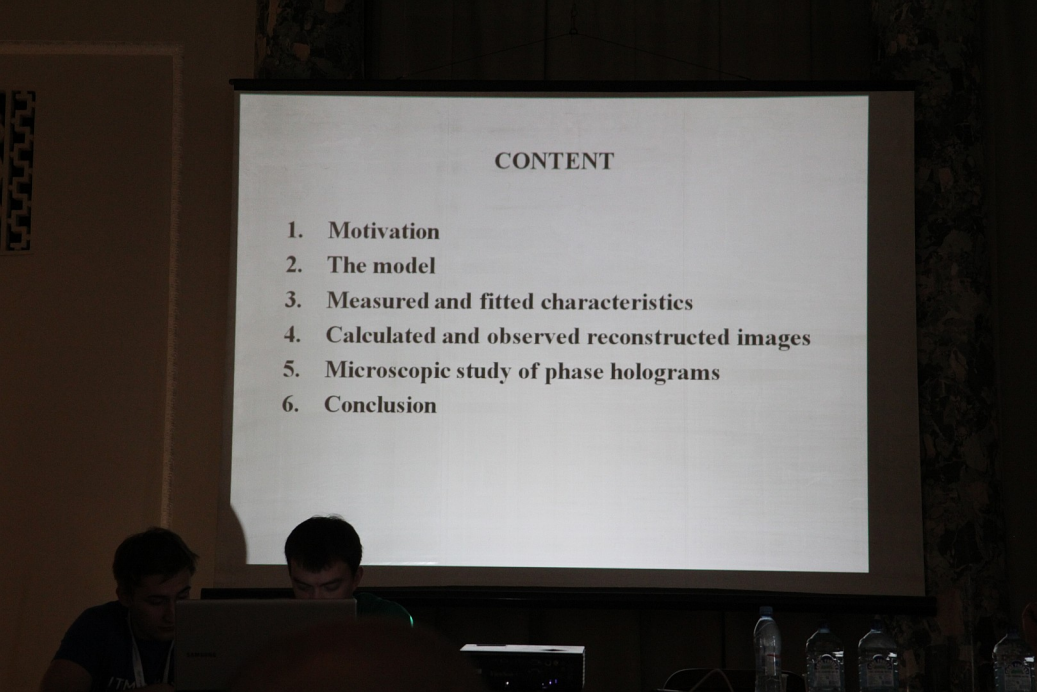
CONTENT
1. Motivation
2. The model
3. Measured and fitted characteristics
4. Calculated and observed reconstructed images
5. Microscopic study of phase holograms
6. Conclusion

1. Motivation

THERE ARE NO PERFECT HOLOGRAMS !!!

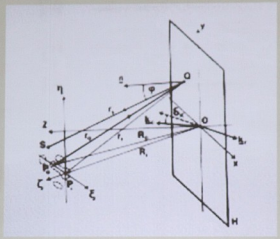

Fig. 1 Holographic reconstruction of the real image a point source. Both reference and reconstruction beams are plane ones. The latter makes a small angle with the conjugate to the reference beam. ABERRATIONS occur, distorting the diffraction limited image.

2. The model

THERE ARE NO PERFECT RECORDING MATERIALS !!!

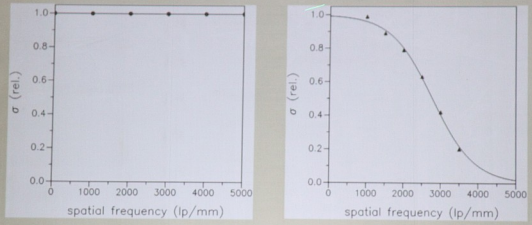

Fig. 2 Modulation transfer function (MTF, square root of the diffraction efficiency of a plane wave hologram *vs.* spatial frequency) of an ideal (left) and real (right) silver halide holographic material (Agfa 8E75). $\nu_0 = 2780$ lp/mm, c = 560 lp/mm, see later.

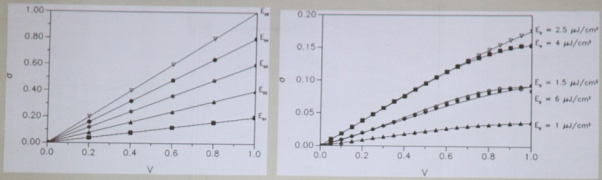

Fig. 3 Lin curves (square root of the diffraction efficiency of a plane wave hologram *vs* bias exposure and fringe visibility) of an ideal (left) and real (right) silver halide holographic material (Agfa 10E70). $\lambda = 632.8$ nm.

MTF of the silver halide recording material:

$$\sigma = \frac{1}{\exp\left(\frac{V - V_0}{c}\right) + 1} \quad (1)$$

Nonlinearity (Lin curves) of the silver halide recording material:

$$\sigma(E_0, V) = f(E_0)(1 - e^{-V}) e^{-\frac{[V - V_0(E_0)]^2}{w^2(E_0)}} \quad (2)$$

$$Par(E_0) = ci_{01}\left(\frac{1}{e^{\frac{ci_{11} - E_0}{ci_{12}}} + 1} + ci_{13}\right)\left(\frac{1}{e^{\frac{E_0 - ci_{21}}{ci_{22}}} + 1} + ci_{23}\right)\left(\frac{1}{e^{\frac{ci_{31} - E_0}{ci_{32}}} + 1} + ci_{33}\right) \quad (3)$$

Where *Par* stands for V_0 and w (27 parameters all !!!).

The effects of the recording material on the reconstructed image can be taken into account in the modified double Fresnel-Kirchhoff integral:

$$I(u,z)=\int_{x_1}^{x_2}\int_{\xi_1}^{\xi_2}\sigma[E_0(x),V(x),\nu(x)]\,G(x)W(x)R(x)O(\xi)\frac{\cos\theta(\xi,x)\cos\rho(x,u,z)}{r_1(\xi,x)\,r_2(x,u,z)}\exp\{ik(r_1-r_2)\}\,d\xi\,dx \qquad (4)$$

where σ is the full effect of the recording material, O , R and W are the complex amplitudes of the object, reference and reconstruction waves G is the distortion caused by the hologram substrate.

Assumptions for the following examples: No angular mismatch at reconstruction, no substrate distortion, $\sigma(E_0, V, \nu) = \sigma_1(E_0, V)\cdot\sigma_2(\nu)$ (i.e. it is separable).

3. Measured and fitted characteristics

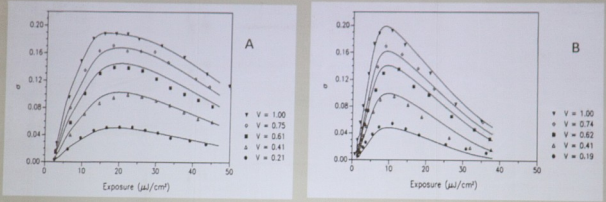

Fig. 4 Measured (symbols) and fitted (lines) Lin curves of Agfa-Gevaert 8E75HD. Amplitude holograms, developer: AAC (A) and Pyrogallol (B). Spatial frequency of the plane wave holograms $\nu = 1200$ lp/mm. $\lambda = 632.8$ nm.

4. Calculated and observed reconstructed images

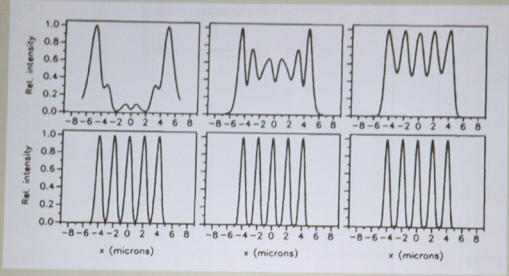

Fig. 5 Calculated reconstructed images of a five-element Ronchi ruling. Only MTF of the recording material was taken into account. Resolution limits (ν_0) are 500, 750, 1000, 1500, 2780 and 4000 lp/mm, respectively. $c = 560 \cdot \nu_0/2780$.

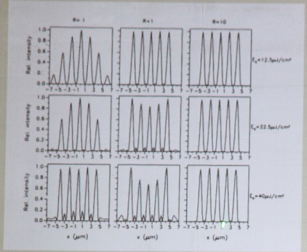

Fig. 6 Calculated reconstructed images of a five-element Ronchi ruling. Only Lin curves (nonlinearity) of the recording material were taken into account. Pyrogallol, R9.

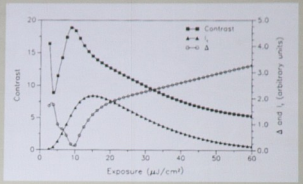

Fig. 7 Contrast, brightness (I_T), contrast and fluctuation (Δ) of the calculated reconstructed image of a five-element Ronchi ruling *vs.* maximum bias exposure. Minimum beam ratio R = 1. Pyrogallol, R9.

Observation of the reconstructed holographic real image of a microscopic test object

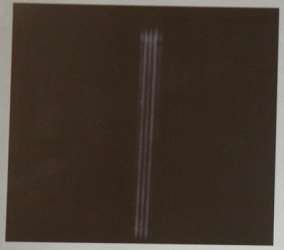

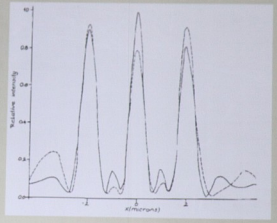

Fig. 8 Reconstructed real image of a three-element Ronchi ruling projected form a microscope (left). Intensity distribution of the same image, and of another one, measured with a moving slit and photomultiplier tube. Agfa-Gevaert 8E75HD, amplitude hologram.

Comparison with the results obtained with coupled wave theory (Credibility test)

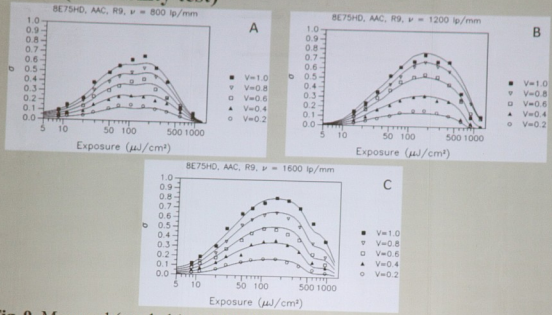

Fig. 9 Measured (symbols) and fitted (lines) Lin curves of Agfa-Gevaert 8E75HD. **Phase holograms**, developer: AAC, Bleach: R9. Spatial frequency of the plane wave holograms ν = 800 lp/mm (A), 1200 lp/mm (B) and 1800 lp/mm (C). λ = 632.8 nm.

$$\sigma(\nu) = \left| \sin \frac{\pi n_1 d}{\lambda \cos\left[\arcsin\left(\frac{\nu\lambda}{2}\right)\right]} \right| \qquad (5)$$

Kogelnik formula

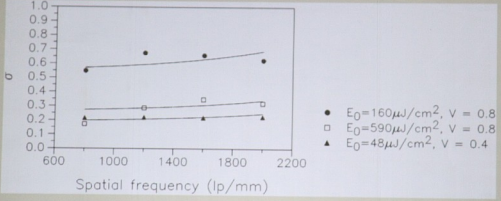

Fig. 10 Square root of the diffraction efficiency vs. spatial frequency of the grating at fixed bias exposure and fringe visibility (both indicated in the graph). Point are measured values. Lines are curves fitted using **Eqs. (2)** and **(3).**

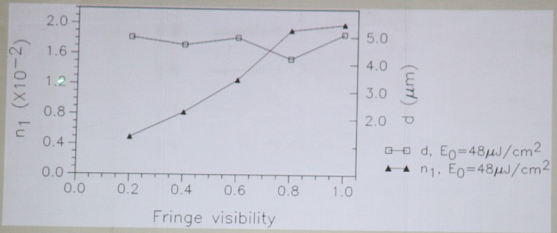

Fig.11 Fitted values of the amplitude of refractive index modulation and hologram thickness vs. fringe visibility at two values of bias exposure at a fixed value of 48 μJ/cm² of bias exposure, using **Eq. 5**.

5. Microscopic study of phase holograms

Phase contrast microscopy: visualization of microscopic phase object by converting optical path length variations into absorption variations across the object. It is achieved by manipulating the image of the object in the Fourier plane (Zernicke, and later Françon).

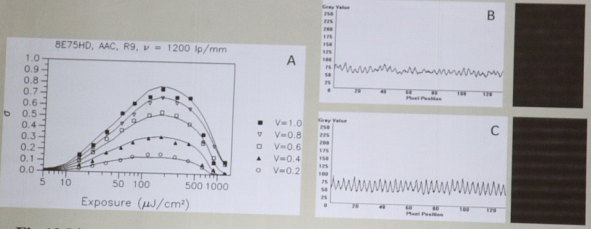

Fig.12 Lin curves of Agfa 8E75HD (A). Phase contrast micrographs of two holograms. (B): point No. 6 of the V= 0.2 curve on (A), and (C): point No. 6 of the V= 1.0 curve on (A) Microscope objective = 100 x, immersion

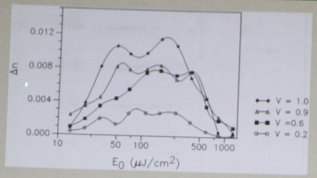

Fig. 13 Measured amplitude of the refractive index modulation vs. bias exposure. 100 X objective. Agfa 8E75HD.

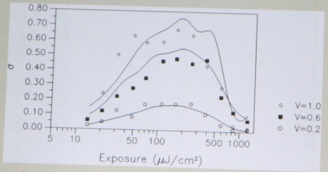

Fig. 14 Measured (lines) and calculated (symbols) values of σ (E_0). Calculations were performed using the measured Δn values and the Kogelnik f[illegible]q. 5).

6. Conclusion

- Resolution and nonlinearity should be taken into account when doing "high-fidelity" holography. This holds true for ALL the holographic recording materials, including dichromated gelatin, photopolymers and CCD (CMOS).
- Characteristics of the holographic recording materials can be modeled, and included in the double Fresnel-Kirchhoff integral - or in other diffraction theories- describing hologram recording and resolution.
- The model enables optimization of the holographic recording parameters (geometry, beam ratio, bias exposure).
- Phase contrast holography can be used for quantitative determination of the amplitude of refractive index modulation of high spatial frequency phase holograms.
- The results were checked using the Kogelnik formula.
- [Results of the Fourier analysis of the grating profiles proved [illegible]ions of the coupled wave theory of volume holograms.]